Special Collection

CO Oxidation on Planar Au/TiO_2 Model Catalysts under Realistic Conditions: A Combined Kinetic and IR Study

Thomas Diemant*[a, b] and Joachim Bansmann*[a]

Dedicated to Prof. Dr. R. Jürgen Behm on the occasion of his 70th birthday

The oxidation of CO on planar Au/TiO_2 model catalysts was investigated under pressure and temperature conditions similar to those for experiments with more realistic Au/TiO_2 powder catalysts. The effects of a change of temperature, pressure, and gold coverage on the CO oxidation activity were studied. Additionally, the reasons for the deactivation of the catalysts were examined in long-term experiments. From kinetic measurements, the activation energy and the reaction order for the CO oxidation reaction were derived and a close correspondence with results of powder catalysts was found, although the overall turnover frequency (TOF) measured in our experiments was around one order of magnitude lower compared to results of powder catalysts under similar conditions. Furthermore, long-term experiments at 80 °C showed a decrease of the activity of the model catalysts after some hours. Simultaneous in-situ IR experiments revealed a decrease of the signal intensity of the CO vibration band, while the tendency for the build-up of side products (e.g. carbonates, carboxylates) of the CO oxidation reaction on the surface of the planar model catalysts was rather low.

1. Introduction

Due to the inertness of bulk gold surfaces,[1] the element gold had been regarded for a long time to be only of minor use in catalytic applications. Accordingly, the catalytic properties of gold catalysts had not been tested very intensively for quite a long time although the few studies on the subject pointed to some catalytic activity for finely dispersed gold particles.[2] Finally, in the late 1980s and the beginning 1990s, Haruta et al. studied the catalytic activity of extremely fine dispersed gold catalysts for the CO oxidation reaction in more detail,[3–5] and observed a surprisingly high activity for samples with gold particles of a mean diameter below 4 nm. This discovery led, in the following years, to a rapid growth of interest in the catalytic properties of gold catalysts and it was found that a wide variety of reactions is catalyzed, including partial or complete oxidation, hydrogenation, water-gas shift reaction, and many others (for reviews see, e.g., ref. [6–10]). Still, most of the work has been focused on the CO oxidation,[11–30] because it can serve as a prototypical model reaction to improve the understanding of the working principles of supported gold catalysts. Besides the interest in the fundamental processes of catalysis, the oxidation of CO on this catalyst material is also interesting from a technical point of view in a number of different possible applications. Supported gold catalysts have been discussed, e.g., for the purification of the feed gas (selective CO oxidation in H_2-rich gas mixtures) of low temperature polymer electrolyte fuel cells (PEFCs),[25,31,32] because they are already very active in the temperature range used for this type of fuel cells.

Besides the extreme importance of the gold particle size on the activity for CO oxidation, studies with disperse gold catalysts revealed that a number of other factors can influence the catalytic activity, e.g., the support material,[5,9] the shape of the gold particles,[9,13] the oxidation state of the gold particles,[33] or the presence of co-adsorbed species.[18,21,24] Unfortunately, also the preparation method and the pretreatment of the gold catalysts before their use in the CO oxidation have a marked influence on the structural properties and the catalytic activity of the disperse catalysts.[17,20] Nevertheless, the underlying reaction mechanism was found to follow a Au-assisted Mars-van Krevelen mechanism, in which only sites directly at or close to the perimeter of Au nanoparticles on TiO_2 participate.[28,30] Similarly, sites at the Au/TiO_2 interface were identified as active sites for O_2 dissociation in DFT calculations.[34]

In order to study the reasons for the enhanced activity of small gold particles and to establish a correlation of the activity with the structural and electronic properties of the catalyst material, the oxidation of CO has also been studied by well-defined planar model catalysts.[35–41] In most of these studies a planar TiO_2 support was chosen, because TiO_2 powders are also for more realistic catalysts one of the most promising supports.[9] As one result of the model studies, the effect of the particle size on the activity was confirmed by the Goodman group[35,36,38] and it was stated that particles with a height of two atomic Au layers have a much higher activity compared to

[a] Dr. T. Diemant, Dr. J. Bansmann
Institut für Oberflächenchemie und Katalyse, Universität Ulm
Albert-Einstein-Allee 47, 89081 Ulm (Germany)
E-mail: thomas.diemant@uni-ulm.de
joachim.bansmann@uni-ulm.de
[b] Dr. T. Diemant
Helmholtz Institute Ulm (HIU) Electrochemical Energy Storage
Helmholtzstraße 11, 89081 Ulm (Germany)

Special Collection An invited contribution to a Special Collection on Interface Phenomena

particles with only one or with three or more layers. Because of the coincidence of the maximum activity with a transition from the metallic to the nonmetallic state, which was derived for particles with two layers from scanning tunneling spectroscopy (STS) measurements, it was concluded that the enhanced activity is triggered by the special electronic properties of these particles. The CO oxidation by gold particles has also been in the focus of theoretical studies, which investigated the reaction with density-functional (DFT) calculations.[42–45] Strain effects,[42,44] the influence of under-coordinated corner atoms on the gold particles, and active sites at the Au–TiO_2 perimeter[34] were pointed out as possible explanations for the particle size effects.

In this publication, we present the results of an extensive combined kinetic and IR study on the CO oxidation by planar Au/TiO_2 model catalysts, which were created by Au deposition on fully oxidized, closed TiO_2 layers on a Ru(0001) substrate (cf. experimental section for more information). We have studied the reaction kinetics of the CO oxidation on these model catalysts under realistic pressure and temperature conditions in detail and are able to present important kinetic factors such as the activation energy for reaction and the reaction order(s). Additionally, the influence of the gold particle size on the catalytic activity was tested, by variation of the deposited gold amount. Finally, the long-time performance and stability of the model catalysts was checked by kinetic and in-situ IR measurements during and XPS measurements before and after this long-term exposure to the reactive gas mixture. The results derived for our model catalyst can be compared to those from powder catalysts, to test if a correlation between both types of catalyst materials exists.

2. Results and Discussion

2.1. Au/TiO_2 Model Catalysts

The structure and chemical composition of the model catalysts were studied by scanning tunneling microscopy (STM) and X-ray photoelectron spectroscopy (XPS) measurements, respectively.

Figure 1 shows exemplarily STM images of model catalyst surfaces with a gold coverage (θ_{Au}) of (a) 0.3 and (b) 0.6 ML. The underlying titania films are rather flat and the gold particles nucleate preferentially at the step defects of the titania substrate.[46] In these two examples, the particles have mean diameters of 2 (0.3 ML Au) and 2.5 nm (0.6 ML Au) and the particle height distribution has its maximum at particles with 3 layers in both cases, although the fraction of higher particles increases from 0.3 to 0.6 ML Au. The tendency to formation of larger gold particles also continues with increasing gold coverage, e.g., at $\theta_{Au}=0.8$ ML, particles with a mean diameter of 3 nm and a height of four to five layers are found. Particles with a height of one atomic layer are only observed at very small Au coverage below 0.1 ML.

The chemical state of the model catalysts was examined using XPS. Figure 2 shows a representative XPS measurement from a model catalyst with 0.43 ML Au. The absence of any

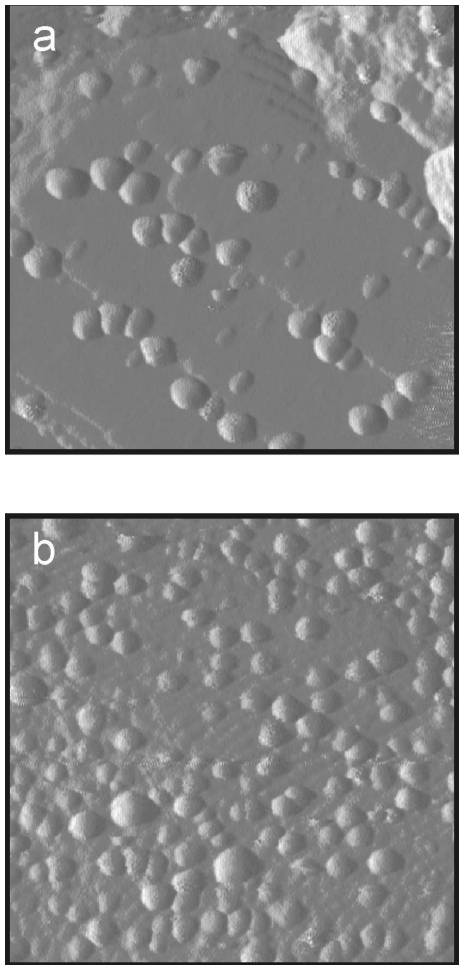

Figure 1. STM images of Au/TiO_2 model catalyst surfaces with different Au coverages (θ_{Au}): a) $\theta_{Au}=0.3$ ML (49×49 nm^2), b) $\theta_{Au}=0.6$ ML (51×51 nm^2). Tunnelling parameters: $U_T=+2.5$ V, $I_T=0.56$ nA. Reprinted with permission from: T. Diemant, Z. Zhao, H. Rauscher, J. Bansmann, R. J. Behm, *Top. Catal.* **2007**, *44*, 83–93. Copyright (2007) Springer Science Business Media, LLC.

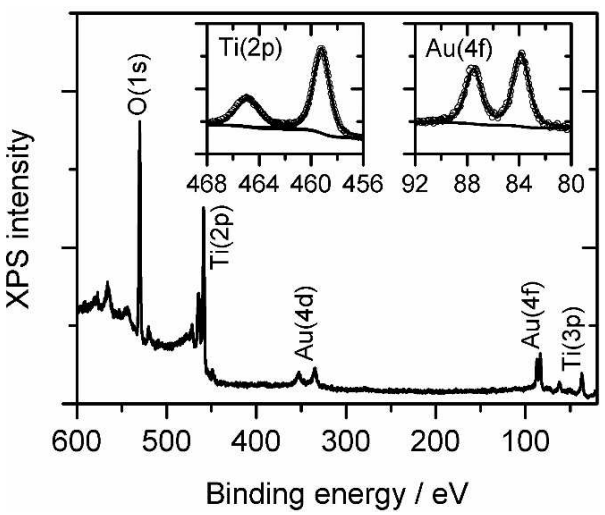

Figure 2. Survey XP spectrum of a Au/TiO_2 model catalyst after preparation ($\theta_{Au}=0.43$ ML). Insets: Detail spectra of the Au(4f) (right) and Ti(2p) (left) region.

contaminations (like C, etc.) is confirmed by the survey spectrum, the insets show detail scans of the Au(4f) and the Ti(2p) region, respectively. Characteristically for fully oxidized Ti atoms in the support (Ti^{4+}),[47] a single doublet with peaks at 459.2 eV ($Ti2p_{3/2}$) and 464.7 eV ($Ti2p_{1/2}$) is sufficient to fit the spectrum in the Ti(2p) region. Similarly, also the Au(4f) spectrum can be fitted by a single peak doublet. The peak position of the Au($4f_{7/2}$) component at 83.9 eV confirms that the gold particles are in the metallic state. These results are in good agreement with values reported in literature for gold particles deposited on TiO_2(110)[48,49] and bulk gold.[50] XPS characterization of the model catalyst samples was always carried out before and after experiments in the high-pressure cell.

2.2. Temperature Dependence of CO Oxidation

Before investigating the activity of the model catalyst, the influence of the sample temperature on the structure of the Au/TiO_2 catalyst was investigated. For this purpose, samples with similar gold loading were heated in 20 mbar of a reactive gas mixture of two parts CO and one part O_2 for three hours to different temperatures between 50 °C and 180 °C. Sintering of the gold particles on the titania substrate should become obvious when comparing XPS measurements before and after gas exposure by a decrease of the intensity of the Au(4f) with respect to the Ti(2p) peaks. Up to temperatures of 130 °C, XPS did not show any decrease of the Au(4f)/Ti(2p) intensity ratio within the error margins of our measurements (approximately 5%). At 150 °C a small decrease of the intensity ratio by 7% was found which increases to 10% at 180 °C. Based on these results it can be concluded that the particle size on the model catalyst was not significantly affected at the applied gas pressure up to 130 °C. On the other hand, several articles reported that the size of the gold particles on TiO_2(110) single crystal substrates was affected under similar conditions even at much lower temperature.[35,36,38] The enhanced stability of the gold particles on our titania films on Ru(0001) compared to TiO_2(110) bulk crystals can partly be explained by the larger roughness of our sample surfaces, leading to a stronger adhesion of the particles on the titania films. Furthermore, UHV-prepared TiO_2(110) crystals are often O-deficient, to ensure sufficient electric conductivity of the crystal for surface analysis techniques. Due to the stronger interaction of gold with the reduced titania substrates, the particle size is smaller on these substrates.[46] The oxidation of the reduced TiO_2(110) substrates under high pressure conditions (in gas mixture containing O_2) could therefore promote sintering of the particles. In contrast, the model catalysts used in our study were already oxidized before the gas exposure and therefore this effect was absent.

In the next step, the dependence of the CO oxidation activity of Au/TiO_2 model catalysts on the temperature was investigated in the temperature range from 50 to 130 °C. At temperatures below 50 °C the activity of the model catalysts was too low to obtain quantitative results. For all experiments shown here, model catalysts with a similar Au coverage between 0.6 and 0.8 ML were used and a gas mixture consisting of two parts of CO and one part of O_2 with a total pressure of 20 mbar was applied. The apparent activation energy for the CO oxidation reaction can be evaluated from Arrhenius type plots as shown in Figure 3b, the TOF values at these temperatures are collected in Table 1. In Figure 3a the increase of the CO_2 concentration in the high-pressure cell, which is operated in the batch mode, is shown. Please note that in the first hours a linear increase of the CO_2 concentration is observed at all reaction temperatures.

The activity of the model catalysts grows with increasing temperature. As shown in Table 1, the TOF increases from 0.07 s^{-1} at 50 °C to 0.48 s^{-1} at 130 °C. Comparison to results of activity measurements with more realistic powder catalysts[51]

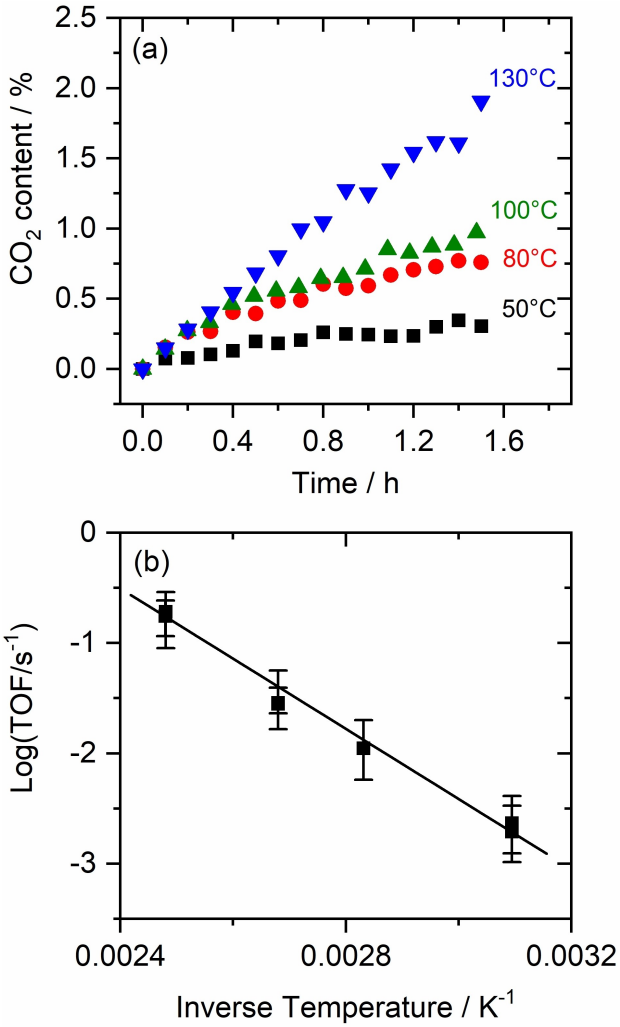

Figure 3. a) Increase of the concentration of CO_2 at different temperatures. b) Arrhenius plot for the determination of the apparent activation energy of CO oxidation.

Table 1. TOF of CO oxidation on Au/TiO_2 model catalysts at different temperature.

Temperature [°C]	50	80	100	130
TOF [s^{-1}]	0.07	0.14	0.21	0.48

indicates that the activity of our model catalyst is one order of magnitude lower under similar pressure and temperature conditions. This discrepancy may be ascribed to the differing structural properties of both types of catalyst materials. From the Arrhenius plot (Figure 3b), the apparent activation energy for the CO oxidation on this model catalyst surface is evaluated to be 27 ± 7 kJ/mole. This value is in excellent agreement with results reported for measurements with Au/TiO_2 powder catalysts, e.g., Schumacher et al.[51] derived the same value when using partial pressures of 10 mbar of CO and O_2 in this temperature range. Additionally, very similar results have been reported by Liu et al.[52] (24 kJ/mole), Bollinger et al.[12] (29 kJ/mole), Cant et al.[53] (32 kJ/mole), and Haruta et al.[5] (34 kJ/mole). Choudhary et al.[20] came to a value of 16 kJ/mole and Lin et al.[54] observed a change of the activation energy from 38 kJ/mol below 360 K to 10 kJ/mole at higher temperature.

2.3. Reaction Orders of the CO Oxidation

In this section, the effect of the total pressure and of the partial pressures of the reactants CO and O_2 on the activity of the Au/TiO_2 model catalysts is discussed. For this purpose, the reaction orders were determined, which give a measure for the influence of the gas pressure on the activity of the catalyst. The reaction orders are derived by a description of the reaction by a simple rate law:

$$R_{CO-Ox} = k \cdot {p_{CO}}^{\alpha_{CO}} \cdot {p_{O_2}}^{\alpha_{O_2}} \quad (1)$$

The exponents α_{CO} and α_{O2} are the reaction orders with respect to the gas components CO and O_2. The overall reaction order α_{Tot} is the sum of these single reaction orders.

$$\alpha_{Tot} = \alpha_{CO} + \alpha_{O_2} \quad (2)$$

The overall reaction order and the reaction orders for both gas components CO and O_2 were determined at 100 °C experimentally. For the overall reaction order, measurements with different total pressure (5 to 50 mbar) but fixed mixing stoichiometry of two parts CO and one part O_2 were conducted. The reaction order was then calculated from the slope of a double-logarithmic plot of the reaction rate versus the total pressure. In this analysis the TOF was used to represent the reaction rate. Similarly, the reaction orders for the gas components CO and O_2 were determined by varying the gas pressure of one gas component while keeping the pressure of the other component fixed. For the CO reaction order, the CO partial pressure was changed from 1.7 to 13.3 mbar while the O_2 partial pressure was kept at 6.7 mbar. For determining the O_2 reaction order, measurements were performed with gas mixtures with an O_2 partial pressure between 6.7 and 53.3 mbar and a constant CO pressure of 13.3 mbar, respectively. The reaction orders were determined analogously to the overall reaction order by a double-logarithmic plot of the reaction rate versus the respective partial pressure.

The development of the reaction rate in dependence of the total pressure and the partial pressures of CO and O_2 are displayed in Figure 4. An increase of the reaction rate is obvious with increasing total pressure (Figure 4a) and with increasing partial pressure of CO (Figure 4b) and O_2 (Figure 4c). In all cases, the increase is linear in the double-logarithmic representation; therefore, the reaction orders can be determined by the slope

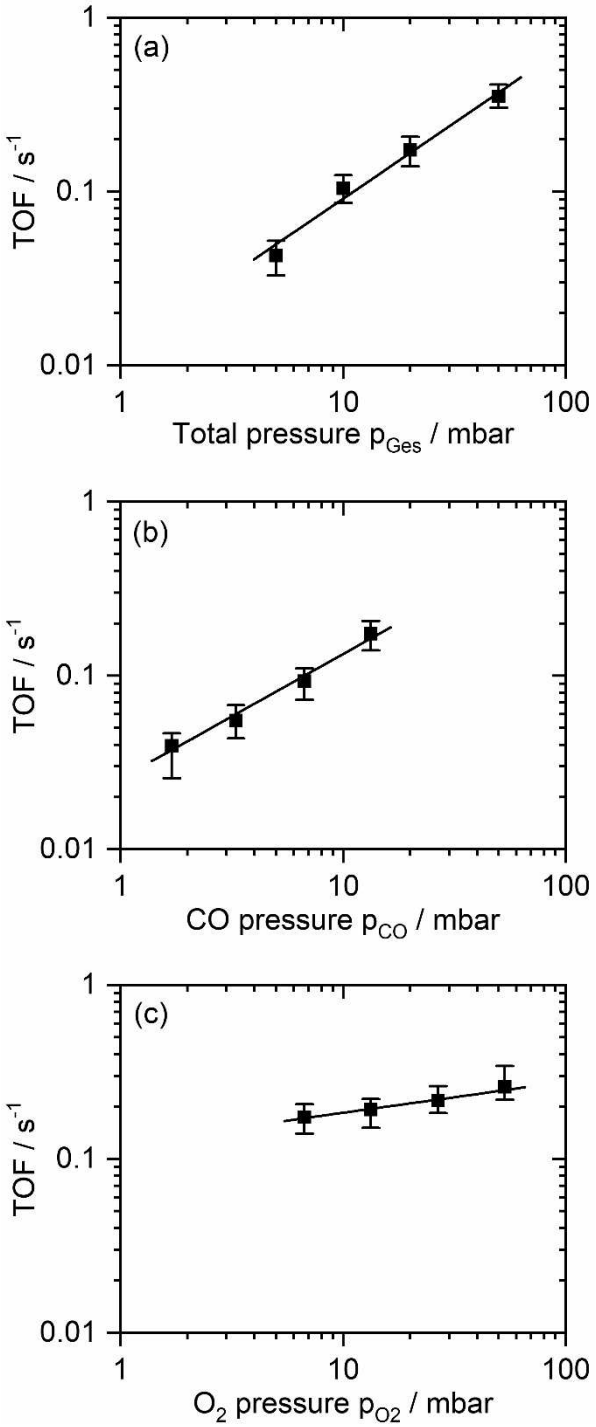

Figure 4. Determination of the reaction orders for the CO oxidation by the Au/TiO_2 model catalysts at 100 °C in CO/O_2 gas mixtures. a) Overall reaction order α_{Tot}, b) CO reaction order α_{CO}, c) O_2 reaction order α_{O2}.

of the three plots. For the overall reaction order α_{Tot} a value of 0.88 ± 0.09 is determined, whereas the CO reaction order α_{CO} is 0.72 ± 0.07 and the O_2 reaction order α_{O2} 0.17 ± 0.05. These experimentally determined values are in line with the expectation that the overall reaction order should be the sum of the reaction orders of the two gas components.

The value of the overall reaction order α_{Tot} of 0.88 indicates that the reaction rate is strongly dependent on the total pressure. Furthermore, the reaction orders α_{CO} and α_{O2} show that the reaction rate mainly depends on the CO partial pressure, whereas the O_2 partial pressure is of smaller importance. For the reaction temperature used throughout these experiments (100 °C), a variation of the CO partial pressure directly results in a change of the CO coverage on the Au particles of the model catalyst, because the adsorption energy of CO is in the range from 65 to 40 kJ/mole. Concomitant IR measurements show that even with a total pressure of 50 mbar the saturation CO coverage is not reached at 100 °C. The high value of the CO reaction order α_{CO} indicates that the reaction rate depends on the CO coverage on the Au particles, which is determined by the adsorption-desorption-equilibrium. In contrast, the O_2 reaction order α_{O2} has a comparatively small value (0.17). As a consequence, it may be assumed that under the reaction conditions used throughout this study the supply of O_2 from the gas phase is not a rate determining step in the reaction mechanism of the CO oxidation.

The values determined in this work for Au/TiO_2 model catalysts can be compared to studies with disperse Au/TiO_2 powder catalysts, to get an impression if the CO oxidation proceeds with a similar reaction mechanism for both types of materials. For differently prepared Au/TiO_2 powder catalysts, the reaction orders for CO and O_2 were reported before in a number of studies under different reaction conditions. Haruta et al.[5] derived values of 0.05 and 0.24 for CO and O_2, respectively, at 20 °C. In contrast, Lin et al.[54] derived at the same temperature for the CO reaction order a value of 0.4, whereas the reactivity was nearly independent of the applied O_2 pressure (O_2 reaction order 0). Bollinger et al.[12] reported values of 0.24 and 0.4 for the CO and O_2 reaction order at 40 °C. Finally, Cant et al.[53] had derived at 47 °C a reaction order of 0.45 for CO and 0.19 for O_2.

The variations observed in this collection of reaction order values from the literature may in part be explained by the differing structural properties of the Au/TiO_2 powder catalysts in these studies. Nevertheless, an influence of the reaction conditions on the reaction order is also obvious. Most prominently, a tendency for an increase of the overall reaction order is observed with increasing temperature. This observation has also been confirmed in a systematic study of the influence of the temperature on the reaction order.[51] Using a gas mixture of one part CO and one part O_2 at 80 °C, an overall reaction order of 0.88 was determined, which increased to 0.95 at 95 °C and further at even higher temperatures. Similarly, an increase of the reaction order was reported before by Bollinger et al. when going from 40 to 80 °C.[12]

The overall reaction order α_{Tot} determined here for a model catalyst is in good agreement with the results of our group on Au/TiO_2 powder catalysts,[51] which were acquired under similar conditions (temperature and gas pressure). From a comparison of the results listed above, it is evident that the increase of the overall reaction order for the Au/TiO_2 powder catalysts is mainly due to the increase of the CO reaction order. Analogous to the model catalysts, the CO coverage also has a strong influence on the reaction rate of the CO oxidation for more realistic powder catalysts. In contrast the O_2 reaction order seems to be quite constant between 0 and 0.4 for powder catalysts in close agreement to the value of 0.17 determined for our Au/TiO_2 model catalyst. In conclusion, it can be noted that under the reaction conditions applied in this study, the CO coverage on the Au particles directly influences the reaction rate of the CO oxidation. In contrast, the O_2 pressure is of smaller importance for the reaction rate. The comparison with Au/TiO_2 powder catalysts shows a close resemblance of the results derived for both types of materials.

2.4. Influence of Gold Coverage on the Activity

The results of a set of experiments to reveal the influence of the gold coverage are displayed in Figure 5. The objective was to study the influence of the Au particle size, which is closely connected to the amount of Au deposited on the surface. The experiments were conducted at a temperature of 100 °C using a reactive gas mixture with a total pressure of 20 mbar and consisting of two parts CO and one part O_2. After deposition of very small gold amounts the rate of CO_2 production was very low, e.g., a sample with 0.03 ML Au showed no difference to the background measurement without any gold on the surface. At this Au coverage, the Au particles consist predominantly of particles with a single Au layer on the titania substrate and have a mean diameter of around 1 nm. After deposition of 0.14 ML Au, a small activity is observed, although the calculated TOF of 0.04 s^{-1} is still very low. At this Au coverage the mean diameter of the particles is about 2 nm and most of them

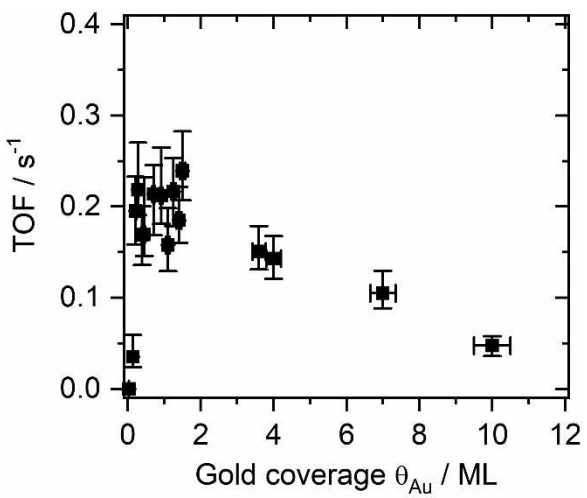

Figure 5. Development of turnover frequency (TOF) on Au/TiO_2 model catalysts at 100 °C with increasing gold coverage.

already consist of two or even three Au layers although a large number of the Au particles still have a height of only one layer. A small increase of the Au coverage to 0.22 ML leads to a considerable increase of the activity. In the coverage range from 0.22 ML to 1.5 ML Au the activity of the samples stays almost constant, with a typical TOF around 0.2 s^{-1}. Within this Au coverage range, the particle diameter increases from 2 nm to 4 nm and the height from mostly three- to four-layered particles to five-or higher-layered particles. Eventually, a further increase of the Au coverage leads to a decrease of the activity. For a model catalyst with 10 ML Au, a TOF of 0.05 s^{-1} is estimated. Since no STM measurements exist for Au coverages above 5 ML, the dispersion was estimated in this range by taking the reciprocal value of the gold coverage, which would hold true for a closed, smooth gold film on the titania substrate. The real dispersion will certainly be higher than the value assumed here, because the XPS results, which show even at 8 ML still the Ti(2p) and O(1s) peak of the titania film, indicate that gold-free areas on the surface exist even at this high gold coverage, which would be also in line with reports in literature,[55] or that at least some areas of the surface are covered only by a very thin gold layer, pointing to a rough gold film. In any case the real dispersion is higher and in turn the TOF is actually smaller than the values reported here.

To summarize, the Au/TiO_2 model catalysts with the highest activity are found for a Au coverage in the range from 0.2 to 1.5 ML and with a mean particle diameter between 2 and 4 nm. Whereas the activity ceases totally for catalysts with smaller Au coverage, samples with higher coverage only show a gradual decrease of the activity. This dependence of the CO oxidation activity on the Au coverage and therefore on the mean Au particle size is in general agreement with studies on realistic powder catalysts[5,13] and planar model catalysts,[35,36] although a significantly stronger dependence of the activity on the particle size was reported for powder catalysts. A comparison with the results of model catalyst studies shows in some parts a different outcome. Regarding the dependence of the activity on the mean particle diameter, our results agree completely with the results of Valden et al.,[35,36] especially with respect to the decrease of the activity for larger gold particles by an order of magnitude. Furthermore, Valden et al.[35,36] proposed that bilayer particles are the most active species which is in contrast to our findings that the activity of the Au particles is of a similar order of magnitude for particles with two to at least five or even six atomic layers of gold. Thus, the concept of an enhancement of the catalytic activity due to the special electronic properties of bilayer Au particles, for which the transition from the non-metallic to the metallic state occurs, cannot explain our results.

2.5. Deactivation Behavior

The results discussed in the preceding sections were based on a calculation of the TOF from the increase of the CO_2 concentration during the first hour of an experiment. In general, within this period a linear increase of the concentration was obtained, as expected for a closed system with a constant reaction rate.

In the next step, the CO_2 partial pressure was recorded for a longer time scale in order to test the long-term activity of the Au/TiO_2 model catalysts. As an example, the evolution of the CO_2 concentration during a long-term experiment of 12 hours is depicted in Figure 6. This experiment was carried out at a temperature of 80 °C using a model catalyst with $\theta_{Au} = 0.7$ ML. Firstly, it can be noted that the CO_2 concentration increases initially almost linearly but that the increase levels off with increasing time and eventually almost ceases at the end of this experiment. As the reaction rate is calculated in this batch-mode experiment from the slope of the increase of the CO_2 concentration, it is obvious that the reaction rate declines more and more with time.

A decrease of the CO oxidation activity of gold catalysts over the reaction time is not exceptional and was observed before in a number of studies with Au/TiO_2 powder catalysts.[12,25,51,56,57] Also in the experiments of the group of Goodman with model catalysts a rapid decrease of the activity was observed already within the first hour of the measurement.[36] Different reasons were proposed to explain the observed deactivation. For Au/TiO_2 powder catalysts, the formation of by-products in the CO oxidation was identified as important source of the deactivation. These by-products such as formates, carbonates, and carboxylates block the active sites of the catalyst and inhibit CO oxidation. The formation of such species is a relatively fast process on Au/TiO_2 powder catalysts under reaction conditions, the presence of such species was usually detected in IR measurements already after minutes.[23,25] In contrast, the decrease of the activity of Au/TiO_2 model catalysts was mainly attributed to the growth of the Au particles in the presence of an oxidizing environment.[35,36]

To test which of the afore-mentioned processes is responsible for the catalyst deactivation, in-situ IR measurements were done in the course of the long-term experiments. The results of a measurement are depicted in Figure 7. The upper spectrum in Figure 7b is the result of an IR measurement at room temper-

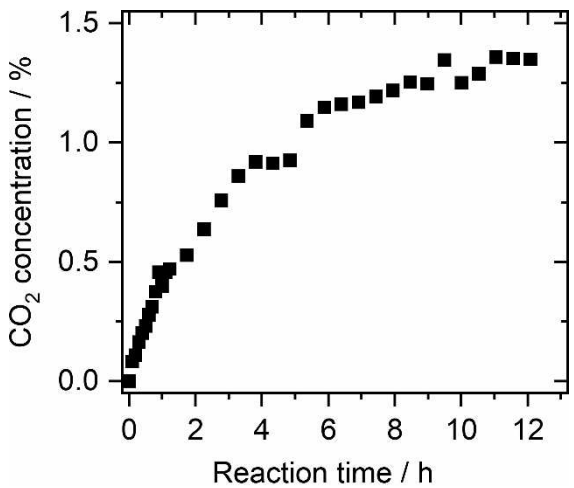

Figure 6. Increase of the CO_2 concentration during a long-term experiment (Au/TiO_2 model catalyst with $\theta_{Au} = 0.7$ ML; 12 h at 80 °C in a mixture of 20 mbar CO/O_2 (2:1)).

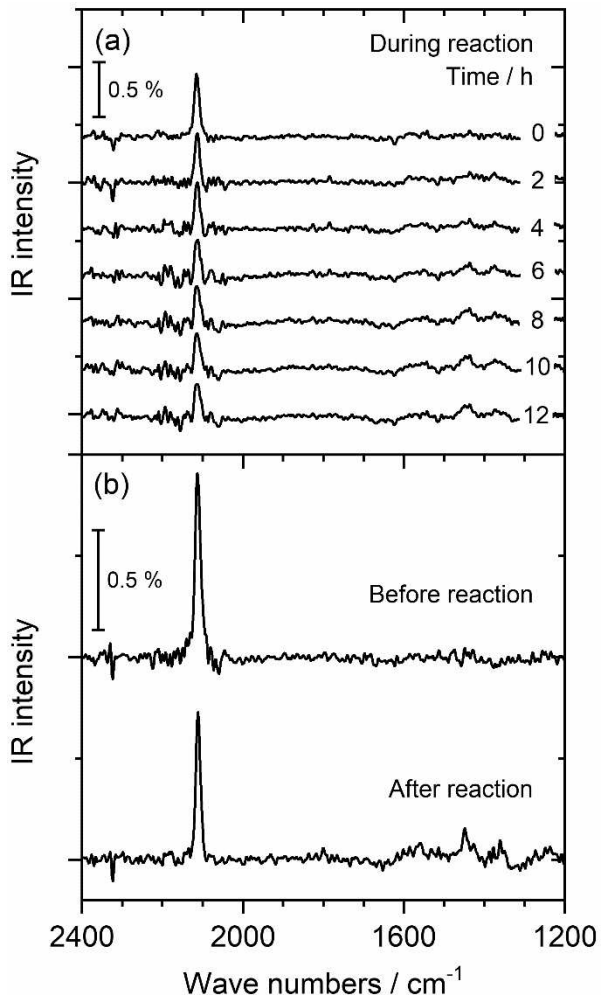

Figure 7. IR measurements of a long-term experiment (12 h at 80 °C in a mixture of 20 mbar CO/O_2 (2:1)). a) IR spectra recorded in the course of the long-term experiment. b) Comparison of IR spectra measured before and after the experiment at room temperature.

ature in the presence of 20 mbar of the gas mixture before the beginning of the actual long-term experiment. In this spectrum a single band is detected at around 2110 cm^{-1}, which can be assigned in agreement with literature[11,12,58] to CO linearly bound on the Au particles. In Figure 7a, IR spectra collected in the course of the long-term experiment are compiled. Due to the higher temperature of 80 °C during these measurements, the IR signal intensity of the band at 2110 cm^{-1} is reduced compared to the result of the measurement at room temperature, pointing to a reduced CO coverage on the Au particles. Furthermore, in the course of the long-term experiment a further significant reduction of the IR intensity is obvious, which is most prominent during the first hours of the experiment. Already for the second IR spectrum in Figure 7a, measured after 2 h reaction time, a decrease of the signal intensity to 2/3 of the initial intensity is noticed and a further slow decrease to 1/2 of the initial intensity after 12 hours is observed in the following measurements. After the long-term experiment the model catalyst was cooled down to room temperature and a further IR spectrum was recorded (Figure 7-Bottom spectrum). Comparison to the spectrum before the long-term experiment shows a noticeable loss of IR signal intensity of around 50% again. This decrease of the IR intensity is indicative for a decrease of the CO coverage on the Au particles under the assumption that the IR signal intensity is linearly connected to the CO coverage, which at least as first order approximation will hold true. This decrease of the steady-state CO coverage on the Au particles may also be of importance in the observed deactivation of the catalysts, because the determination of the pressure dependence of the reaction rate showed a strong influence of the equilibrium CO coverage on the activity.

The observed decrease of the IR intensity can be caused by different reasons. Firstly, the surface of the model catalyst might get blocked by co-adsorbed impurities, which are collected in the course of the experiment, or similarly due to the formation of by-products of the CO oxidation, which can prevent CO adsorption on the surface. Indeed, for Au/TiO_2 powder catalysts a fast formation of diverse by-products of the CO oxidation was commonly observed under the conditions of the CO oxidation. Formates, carbonates, and carboxylates were instantaneously detected after the contact of the catalyst material with the reactive gas mixture.[11,23,25] The presence of these species is evidenced by a number of different IR bands in the wave number range from 1700 to 1300 cm^{-1}. In contrast to powder catalysts, Figure 7 demonstrates that our model catalyst only shows a minor tendency to the formation of these by-products. In the IR spectrum collected after the long-term experiment (Figure 7b – Bottom spectrum) only very weak bands are observed in this wave number range. In principle, three different broad bands can be distinguished in this spectrum, which appear at 1560, 1445, and 1360 cm^{-1}. The relatively weak band at 1560 cm^{-1} is assigned in correspondence with literature[12,59,60] to carbonate groups bound with two O atoms to one Ti^{4+} center. The signal with the strongest intensity at 1445 cm^{-1} can be ascribed to carbonate groups bound with a single O atom to the surface.[60,61] Bands at 1360 cm^{-1} were assigned in literature either also to twofold bound carbonate groups or to formates on the surface.[12,60,61] The sluggish growth of these bands in the course of the long-term experiment (Figure 7a) shows, that the formation of these species is a relatively slow process. The IR spectrum recorded after the first two hours of the experiment shows none of the described bands, a result contradictory to the assumption that the decrease of the CO coverage on the Au particles is caused by a blockage of the catalyst surface by these side-products. In any case, it is worth to mention that in contrast to powder catalysts only a small tendency for the formation of these by-products is observed for the model catalysts. This difference can be explained by the differing structural properties of powder and model catalysts, with a much higher number of defect sites in the support material for the disperse powder catalysts. Besides, the tendency for the formation of side-products seems to be also influenced by the presence of co-adsorbed species. It has been reported in literature before that, e.g., hydroxyl groups accelerate the formation of the by-products.[11] Indeed, hydroxyl groups are still present on the catalyst surface even after a

calcination step in the catalyst conditioning procedure for most powder catalysts.[26] In contrast, for the model catalysts the surface is at least in the beginning of the experiments anhydrous.

The reduction of the IR intensity might also be caused by a growth of the Au particles during the long-term experiment since larger Au particles have a smaller dispersion, i.e., less adsorption sites (per total Au atom number). Furthermore, the CO binding strength decreases on larger Au particles and thus, under the equilibrium conditions of the experiments reported here, a further decrease of the CO coverage on the Au particles would be expected upon particle growth. However, the experiments presented in part 2.1 of this paper had shown that a significant sintering of the Au particles after three hours of exposure to a gas mixture with the same total pressure and the same composition only appears at temperatures of 150 °C and above. Therefore, it can be excluded that sintering plays a major role in this process, because the most significant decrease of the IR intensity is already observed within the initial two hours of the long-term experiment.

As a final possible explanation, it can be argued that instead of a sintering and growth of the Au particles only an internal modification of the Au particles occurs in the course of the experiment. As the preparation of the Au particles was carried out in the UHV section at room temperature, it is reasonable to assume that the perfection of the faceting of the Au particles is improved during the course of the experiment.

With this modification under-coordinated defect places on the Au particles, where CO is bound more strongly, cease to exist, resulting in a reduction of the overall CO coverage on the Au particles.

To probe the changes of the chemical and structural properties of the model catalysts after the long-term experiment in more detail, XPS measurements were conducted after the transfer of the sample from the reaction cell back to the UHV section of the system. The survey spectrum of a Au/TiO_2 model catalyst with a gold coverage of around 0.9 ML, which was subjected to a long-term experiment analogous to the one described before, is shown in Figure 8. The spectrum shows that no major contaminations can be detected on the surface.

The insets of Figure 8 display detail spectra of the C(1s) and the Ni(2p) regions, respectively. The detail spectrum in the C(1s) region was recorded to get more information about the type and amount of C-containing species, which were collected on the surface in the course of the long-term experiment. In this scan two broad peaks at around 285 and 289 eV are detected. The first peak is assigned to graphitic/carbonaceous impurities. The second feature is caused by species like carbonates, which contain besides carbon also oxygen. From the intensity of this two peaks it can be deduced, that the amount of C-containing species on the surface of the model catalyst is relatively small, even when taking into account the low sensitivity of XPS for C in comparison to other elements. Finally, contamination of the surface by nickel can be excluded considering the detail scan in the Ni(2p) region. Metallic nickel deposits are the product of the decomposition of nickel carbonyls, which can be formed at high CO pressure by reaction of CO with the stainless steel

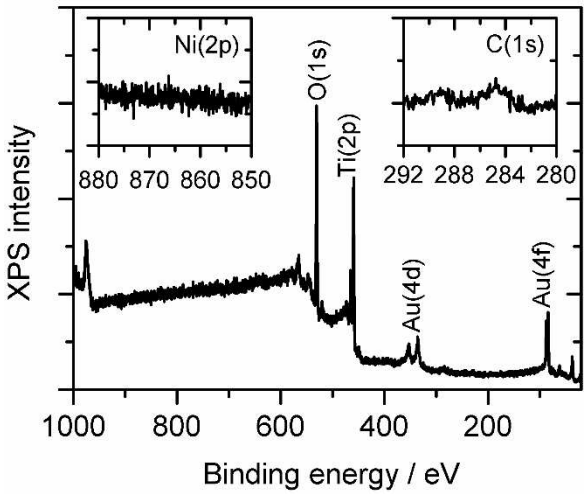

Figure 8. Survey XP spectrum of a Au/TiO_2 model catalyst with $\theta_{Au} = 0.9$ ML after a long-term experiment (12 h at 80 °C in a mixture of 20 mbar CO and oxygen (2:1)). Insets: Detail spectra of the C(1s) (left panel) and the Ni(2p) region (right panel).

vessel, if no precautions are taken to omit this possibility.[62] It turned out, that under our experimental conditions the deposition of nickel on the model catalyst surface remains below the detection limit of the XPS measurement.

The XP detail spectra in the Au(4f), Ti(2p), and O(1s) region taken before and after the long-term experiment are collected in Figure 9. The comparison of the scans in the Au(4f) region shows that they are essentially identical. Similar to the measurement before the long-term experiment the spectrum recorded after the experiment can still be fitted by one peak set, and the $Au(4f_{7/2})$-peak is located at 83.9 eV pointing to the persistence of metallic gold particles.

Similarly, a comparison of the scans in the Ti(2p) region indicates that no major changes of the state of the Ti atoms in the TiO_2 model catalyst support occurred. A set of two peak components is sufficient to fit the experimental result and the position of the $Ti(2p_{3/2})$-peak at 459.2 eV confirms the oxidation state to be Ti^{4+}. When comparing the ratio of the integrated signal intensities of the Au(4f) and the Ti(2p) peaks before and after reaction, a possible sintering in the course of the experiment could be identified by a decrease of this ratio. The absence of any significant change of this ratio confirms that at least no pronounced growth of the Au particles has occurred.

In conclusion, we propose that the decrease of the steady-state CO coverage can be explained as follows: Since a pronounced sintering of the gold particles can be excluded and the formation of by-products of the CO oxidation is not detectable during the first hours of the long-term experiment it can be assumed that the strong decrease of the IR intensity in the first hour is mainly caused by an increase of the internal ordering of the Au particle facets. We do not exclude that the number of very small Au particles with only a few atoms will significantly decrease during reaction and this effect may contribute as well to the initial deactivation. The onset of the formation of side-products after some hours might then be

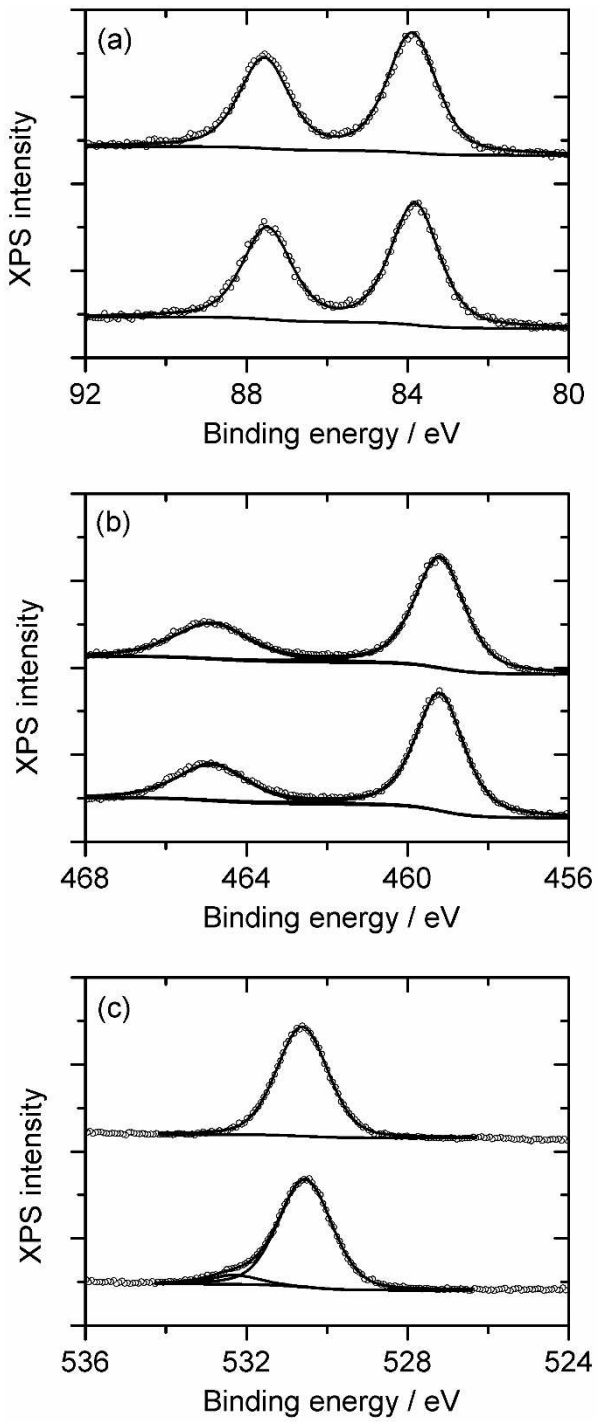

Figure 9. Comparison of detail XP spectra from a Au/TiO_2 model catalyst with $\theta_{Au} = 0.9$ ML before and after a long-term experiment (12 h at 80 °C in a mixture of 20 mbar CO and oxygen (2:1)). a) Au(4f) region; b) Ti(2p) region; (c) O(1s) region.

responsible for the observed further slight decrease of the IR intensity during this time period.

In contrast to the detail spectra in the Au(4f)- and Ti(2p)-region, a comparison of the results of the measurements in the O(1s) region shows the formation of a new component after the long-term experiment. This component is detected at higher binding energies compared to the original peak and has around 10% of the intensity of the main peak. While the main component is still centered at 530.5 eV the additional component is found at 532.2 eV. The additional component is caused by O-containing species, which are accumulated during the long-term experiment on the surface of the model catalyst. To clarify the origin of the additional component in the O(1s) spectrum of the XPS measurement, a temperature-programmed desorption (TPD) experiment (not shown for sake of brevity) was conducted under UHV conditions. In this experiment, CO_2 and H_2O were identified as main desorption products, whereby H_2O dominates over CO_2 by around three times in intensity. In contrast, evolution of O_2 from the surface is not detected until the end of the temperature ramp at 750 K. It is clear that the CO_2 is produced by the decomposition of carbonates and carboxylates during the TPD run. From TPD experiments under UHV conditions, it is known that H_2O should not stay adsorbed/desorb from a $TiO_2(110)$ surface[63,64] at room temperature, whereas OH is more strongly bound and is still present. Therefore, it can be assumed that hydroxyl groups, which may form during the reaction experiments due to the presence of trace amounts (~2 ppm) of H_2O in the reactive gas mixture, remain on the sample under UHV conditions and are detected in the XPS measurements. These results demonstrate that hydroxyl groups are also formed besides carbonates on the surface of the model catalyst during the long-term experiment.

3. Conclusions

The catalytic activity of Au/TiO_2 model systems was probed using the CO oxidation as test reaction. The Au particles of the model catalyst are not very susceptible to a sintering; up to 130 °C no significant particle growth is observed in 20 mbar of a gas mixture of CO and O_2. In the kinetic measurements, the activation energy for CO oxidation (27 kJ/mole) and the overall reaction order ($\alpha_{Tot} = 0.88$) and the reaction orders for both gas components ($\alpha_{CO} = 0.72$, $\alpha_{O2} = 0.17$) were determined. These values are in close agreement with the results of studies with more realistic powdered Au/TiO_2 samples although the overall reactivity is one order of magnitude lower for the model catalysts. The close correspondence demonstrates that the oxidation of CO proceeds with a similar reaction mechanism for both types of catalyst materials. Furthermore, the dependence of the CO oxidation activity on the Au coverage, and connected with this the Au particle size, was studied. A very small activity was observed for samples with Au particles of a height of only one Au layer. After the formation of higher Au particles, with at least two or three layers, a sudden increase of the activity was observed. Eventually, for larger gold particles, exceeding six or seven Au layers, again a gradual decrease of the activity could be noted.

In the long-term experiments a marked decrease of the CO oxidation activity and at the same time a decrease of the steady-state CO coverage on the model catalyst surface was evidenced. These results may in part be due to an increasing ordering of the gold particles under the reaction conditions

employed in these experiments. A strong influence of particle sintering can be excluded on the basis of the ex-situ XPS measurements, which show a constant Au(4f)/Ti(2p) intensity ratio. Additionally, in comparison to more realistic powdered Au/TiO_2 samples the tendency for the formation and collection of by-products of the CO oxidation (formates, carbonates, carboxylates) on the catalyst surface is for the planar model catalysts rather low, leading to the sporadic formation of carbonates on the surface. Instead, in the course of the long-term experiments H_2O, which was present in trace amounts in the gas atmosphere, leads to the formation of hydroxyl groups on the surface of the model catalyst. It remains an open question, why the hydroxyl groups do not have a promotional effect on the CO oxidation activity, as it was observed for powdered catalysts, although it may be assumed that the beneficial effect arising from a hydroxylation of the sample surface is overcompensated by the negative effect due to the restructuring of the Au particles.

Experimental Section

The experiments reported in this study were done in two separate UHV systems. The first of these systems was used for scanning tunneling microscopy (STM) measurements and featured, besides a home-built single tube STM, standard facilities for surface preparation and characterization. The second system was equipped with a reaction cell in which the kinetic and infrared measurements were carried out, for details, see.[65] Briefly, the UHV section of this system contained standard facilities for sample preparation, a quadrupole mass spectrometer for residual gas analysis and temperature-programmed desorption (TPD) measurements, and facilities for x-ray photoelectron spectroscopy (XPS). It was used for the preparation of model catalyst samples and their analysis before and after the experiments in the reaction cell. The reaction cell had facilities for kinetic measurements (differentially pumped mass spectrometer) and IR experiments. For IR measurements in the reflection-absorption mode two CF16 connections, equipped with home-built vacuum tight KBr windows, were used.

A Ru(0001) single crystal was used as substrate for the Au/TiO_2 model catalysts in both UHV systems. Temperature measurement was accomplished by a type-C thermocouple fixed to the crystal. Titania films of around 10 monolayer equivalent (MLE) thickness were prepared on these substrates by deposition of titanium at 640 K in an atmosphere of $2\cdot10^{-7}$ mbar oxygen with a deposition rate yielding around 0.5 MLE/minute. One monolayer equivalent (MLE) is defined as the amount of titania necessary to completely cover the Ru(0001) surface by one layer. After this procedure, the titania films are not fully oxidized[46] and were thus treated in $2\cdot10^{-6}$ mbar oxygen firstly for 15 minutes at 800 K, subsequently at 1000 K for one minute, and finally at 950 K for another minute. After this procedure the oxygen pressure was maintained during the cooling down of the samples for another 5 minutes, resulting in fully oxidized titania films, as evidenced by XPS measurements. The film growth during Ti deposition can be characterized by a Stranski-Krastanov growth mode, with big TiO_x islands on the 1 ML TiO_2.[66] The oxidative annealing steps lead to a complete oxidation and smoothing of the layer, the TiO_2 terraces show on top a structure equivalent to $TiO_2(110)$-(1×1) surface. The formation of a closed and relatively smooth TiO_2 layer is confirmed by the absence of the Ru 3d peak in XPS. In the following, gold deposition was carried out with a rate of around 0.05 ML/min at room temperature. The Au coverage is referred to a pseudomorphic overlayer on the Ru(0001) substrate in this publication, i.e., $1.6\cdot10^{15}$ Au atoms/cm^2.

The STM images were recorded at positive sample bias voltages (+ 2.0 V–2.5 V) in a constant current mode (0.56 nA). Careful analysis of the STM measurements lead to detailed information about the morphology of the gold particles.[66] Using this information we were able to calculate the decrease of the dispersion of the Au particles (fraction of atoms on the surface divided by the total number of atoms in the particle) with increasing nominal Au coverage, a prerequisite to determine the turn-over frequency (TOF), i.e., the number of reacted CO molecules per second and Au atoms on the surface of the particle. It has to be noted, that the tendency of the model catalysts to form superposed or merged gold particles at very high gold coverage, makes the determination of a precise value for the dispersion in this coverage range difficult.

For the kinetic measurements in the reaction cell, a differentially pumped mass spectrometer was used to analyze the temporal evolution of the gas composition. In the experiments, both sides of the Ru(0001) single crystal were covered with a titania film, because ruthenium or, more precisely, RuO_2 (possibly formed under reaction conditions), is known to catalyze the oxidation of CO.[67,68] Background measurements using samples with a titania film on both sides but without any gold deposition showed anyway a measurable increase of the CO_2 concentration, although in literature it has been reported that pure titania without gold has no activity for the CO oxidation reaction.[69] This activity can presumably be ascribed to the edge of the Ru(0001) single crystal, which was not covered by the TiO_2 film. To account for the background activity, measurements with gold-free samples were performed for each set of reaction parameters (temperature, total pressure, gas composition) and the measurements with gold-covered samples were corrected with respect to this effect. In this study, samples with gold deposited on both sides of the crystal were used to enhance the CO_2 production. Based on the knowledge of the dispersion determined from STM measurements, the TOF was calculated.

Infrared reflection absorption spectroscopy (IRAS) measurements using a Bruker Tensor 27 spectrometer were performed to study in-situ the adsorbed species on the surface of the model catalyst during the reaction experiments. The IR technique is especially well-suited for experiments at elevated pressure due to relatively small absorption effects in the gas phase when sufficiently short beam paths are used.[70] Nevertheless, the IR measurements are influenced by the absorption of gas phase CO at a pressure above 1 mbar. Polarization modulation (PM) technique was used throughout the IR measurements of this study to eliminate the unwanted gas phase contribution; details of the PM technique have already been described elsewhere.[71,72] Before polarizing the IR beam by a ZnSe wire grid polarizer, it is focused by a concave mirror on the sample, and then reflected by the sample onto a Mercury–Cadmium–Telluride (MCT) detector. The direction of polarization is constantly modulated between p- and s-polarization by a photoelastic modulator unit (PEM, Hinds Instruments, II/ZS37).

XP spectra were recorded at room temperature using non-monochromatized Al-K_α radiation for excitation and a hemispherical sector analyzer operated in the fixed transmission mode at pass energies of 20 eV and 50 eV for detail and survey scans, respectively. After subtracting a Shirley background, the peaks were fitted using a nonlinear least squares routine with mixed Gaussian-Lorentzian peak characteristics.

Acknowledgements

This work was supported by the Deutsche Forschungsgemeinschaft within the Schwerpunktprogramm 1091 (Be1201/9-5) and by the Landesstiftung Baden-Württemberg within the "Kompetenznetz Funktionelle Nanostrukturen" (Sub-project C6). The authors would like to thank Dr. Zhong Zhao for providing the STM data. Open access funding enabled and organized by Projekt DEAL.

Conflict of Interest

The authors declare no conflict of interest.

Keywords: deactivation · gold · heterogeneous catalysis · kinetics · titania

[1] B. Hammer, J. K. Nørskov, *Nature* **1995**, *376*, 238.
[2] D. Y. Cha, G. Parravano, *J. Catal.* **1970**, *18*, 200.
[3] M. Haruta, T. Kobayashi, H. Sano, N. Yamada, *Chem. Lett.* **1987**, *16*, 405.
[4] M. Haruta, N. Yamada, T. Kobayashi, S. Iijima, *J. Catal.* **1989**, *115*, 301.
[5] M. Haruta, S. Tsubota, T. Kobayashi, H. Kageyama, M. J. Genet, B. Delmon, *J. Catal.* **1993**, *144*, 175.
[6] M. Haruta, *Catal. Today* **1997**, *36*, 153.
[7] G. C. Bond, D. T. Thompson, *Catal. Rev. Sci. Eng.* **1999**, *41*, 319.
[8] G. C. Bond, D. T. Thompson, *Gold Bull.* **2000**, *33*, 41.
[9] M. Haruta, *CATTECH* **2002**, *6*, 102.
[10] D. A. Panayotov, J. R. Morris, *Surf. Sci. Rep.* **2016**, *71*, 77.
[11] F. Boccuzzi, A. Chiorino, S. Tsubota, M. Haruta, *J. Phys. Chem.* **1996**, *100*, 3625.
[12] M. A. Bollinger, M. A. Vannice, *Appl. Catal. B* **1996**, *8*, 417.
[13] G. R. Bamwenda, S. Tsubota, T. Nakamura, M. Haruta, *Catal. Lett.* **1997**, *44*, 83.
[14] M. A. P. Dekkers, M. J. Lippits, B. E. Nieuwenhuys, *Catal. Lett.* **1998**, *56*, 195.
[15] F. Boccuzzi, G. Cerrato, F. Pinna, G. Strukul, *J. Phys. Chem. B* **1998**, *102*, 5733.
[16] F. Boccuzzi, A. Chiorino, *J. Phys. Chem. B* **2000**, *104*, 5414.
[17] F. Boccuzzi, A. Chiorino, M. Manzoli, P. Lu, T. Akita, S. Ichikawa, M. Haruta, *J. Catal.* **2001**, *202*, 256.
[18] M. Daté, M. Haruta, *J. Catal.* **2001**, *201*, 221.
[19] F. Boccuzzi, A. Chiorino, M. Manzoli, *Surf. Sci.* **2002**, *502/503*, 513.
[20] T. V. Choudhary, C. Sivadinarayana, C. C. Chusuei, A. K. Datye, J. P. Fackler, D. W. Goodman, *J. Catal.* **2002**, *207*, 247.
[21] H. H. Kung, M. C. Kung, C. K. Costello, *J. Catal.* **2003**, *216*, 425.
[22] M. Manzoli, A. Chiorino, F. Boccuzzi, *Surf. Sci.* **2003**, *532–535*, 377.
[23] B. Schumacher, V. Plzak, M. Kinne, R. J. Behm, *Catal. Lett.* **2003**, *89*, 109.
[24] M. Daté, M. Okumura, S. Tsubota, M. Haruta, *Angew. Chem.* **2004**, *116*, 2181, *Angew. Chem. Int. Ed.* **2004**, *43*, 2129.
[25] B. Schumacher, Y. Denkwitz, V. Plzak, M. Kinne, R. J. Behm, *J. Catal.* **2004**, *224*, 449.
[26] B. Schumacher, V. Plzak, J. Cai, R. J. Behm, *Catal. Lett.* **2005**, *101*, 215.
[27] B.-K. Chang, B. W. Jang, S. Dai, S. H. Overbury, *J. Catal.* **2005**, *236*, 392.
[28] D. Widmann, R. J. Behm, *Angew. Chem.* **2011**, *123*, 10424, *Angew. Chem. Int. Ed.* **2011**, *50*, 10241.
[29] J. Saavedra, C. Powell, B. Panthi, C. J. Pursell, B. D. Chandler, *J. Catal.* **2013**, *307*, 37.
[30] D. Widmann, R. J. Behm, *Acc. Chem. Res.* **2014**, *47*, 740.
[31] M. J. Kahlich, H. A. Gasteiger, R. J. Behm, *J. Catal.* **1999**, *182*, 430.
[32] C. Rossignol, S. Arrii, F. Morfin, L. Piccolo, V. Caps, J.-L. Rousset, *J. Catal.* **2005**, *230*, 476.
[33] Q. Fu, H. Saltsburg, M. Flytzani-Stephanopoulos, *Science* **2003**, *301*, 935.
[34] Z. Duan, D. Henkelman, *ACS Catal.* **2011**, *5*, 1589.
[35] M. Valden, X. Lai, D. W. Goodman, *Science* **1998**, *281*, 1647.
[36] M. Valden, S. Pak, X. Lai, D. W. Goodman, *Catal. Lett.* **1998**, *56*, 7.
[37] V. A. Bondzie, S. C. Parker, C. T. Campbell, *Catal. Lett.* **1999**, *63*, 143.
[38] C. C. Chusuei, X. Lai, K. Luo, D. W. Goodman, *Top. Catal.* **2001**, *14*, 71.
[39] M. S. Chen, D. W. Goodman, *Science* **2004**, *306*, 252.
[40] O. Meerson, G. Sitja, C. R. Henry, *Eur. Phys. J. D* **2005**, *34*, 119.
[41] I. Laoufi, M.-C. Saint-Lager, R. Lazzari, J. Jupille, O. Robach, S. Garaudee, G. Cabailh, P. Dolle, H. Cruguel, A. Bailly, *J. Phys. Chem. C* **2011**, *115*, 4673.
[42] M. Mavrikakis, P. Stoltze, J. K. Nørskov, *Catal. Lett.* **2000**, *64*, 101.
[43] N. Lopez, J. K. Nørskov, *J. Am. Chem. Soc.* **2002**, *124*, 11262.
[44] Y. Xu, M. Mavrikakis, *J. Phys. Chem. B* **2003**, *107*, 9298.
[45] N. Lopez, T. V. W. Janssens, B. S. Clausen, Y. Xu, M. Mavrikakis, T. Bligaard, J. K. Nørskov, *J. Catal.* **2004**, *223*, 232.
[46] Z. Zhao, T. Diemant, D. Rosenthal, K. Christmann, J. Bansmann, H. Rauscher, R. J. Behm, *Surf. Sci.* **2006**, *600*, 4992.
[47] U. Diebold, *Surf. Sci. Rep.* **2003**, *48*, 53.
[48] L. Zhang, R. Persaud, T. E. Madey, *Phys. Rev. B* **1997**, *56*, 10549.
[49] S. Kielbassa, M. Kinne, R. J. Behm, *J. Phys. Chem. B* **2004**, *108*, 19184.
[50] M. P. Seah, G. C. Smith, M. T. Anthony, *Surf. Interface Anal.* **1990**, *15*, 293.
[51] B. Schumacher, Ph.D. Thesis, Ulm University, **2005**.
[52] H. Liu, A. I. Kozlov, A. P. Kozlova, T. Shido, K. Asakura, Y. Iwasawa, *J. Catal.* **1999**, *185*, 252.
[53] N. W. Cant, N. J. Ossipoff, *Catal. Today* **1997**, *36*, 125.
[54] S. D. Lin, M. Bollinger, M. A. Vannice, *Catal. Lett.* **1993**, *17*, 245.
[55] L. Zhang, F. Cosandey, R. Persaud, T. E. Madey, *Surf. Sci.* **1999**, *439*, 73.
[56] M. M. Schubert, V. Plzak, J. Garche, R. J. Behm, *Catal. Lett.* **2001**, *76*, 143.
[57] R. Zanella, S. Giorgio, C.-H. Shin, C. R. Henry, C. Louis, *J. Catal.* **2004**, *222*, 357.
[58] J. France, P. Hollins, *J. Electron Spectrosc. Relat. Phenom.* **1993**, *64/65*, 251.
[59] F. Boccuzzi, S. Tsubota, M. Haruta, *J. Electron Spectrosc. Relat. Phenom.* **1993**, *64/65*, 241.
[60] L.-F. Liao, C.-F. Lien, D.-L. Shieh, M.-T. Chen, J.-L. Lin, *J. Phys. Chem. B* **2002**, *106*, 11240.
[61] J.-D. Grunwaldt, M. Maciejewski, O. S. Becker, P. Fabrizioli, A. Baiker, *J. Catal.* **1999**, *186*, 458.
[62] D. E. Starr, S. K. Shaikhutdinov, H.-J. Freund, *Top. Catal.* **2005**, *36*, 33.
[63] M. B. Hugenschmidt, L. Gamble, C. T. Campbell, *Surf. Sci.* **1994**, *302*, 329.
[64] M. A. Henderson, *Surf. Sci.* **1996**, *355*, 151.
[65] Z. Zhao, T. Diemant, T. Häring, H. Rauscher, R. J. Behm, *Rev. Sci. Instrum.* **2005**, *76*, 123903.
[66] Z. Zhao, Ph.D. Thesis, Ulm University, **2006**.
[67] H. Over, Y. D. Kim, A. P. Seitsonen, S. Wendt, E. Lundgren, M. Schmid, P. Varga, A. Morgante, G. Ertl, *Science* **2000**, *287*, 1474.
[68] H. Over, M. Muhler, *Prog. Surf. Sci.* **2003**, *72*, 3.
[69] F. Cosandey, T. E. Madey, *Surf. Rev. Lett.* **2001**, *8*, 73.
[70] G. Rupprechter, *Annu. Rep. Prog. Chem. Sect. C* **2004**, *100*, 237.
[71] M. J. Green, B. J. Barner, R. M. Corn, *Rev. Sci. Instrum.* **1991**, *62*, 1426.
[72] B. Wang, *Spectroscopy* **1997**, *12*, 30.

Manuscript received: November 20, 2020
Revised manuscript received: January 4, 2021
Accepted manuscript online: January 7, 2021
Version of record online: February 11, 2021